Published in final edited form as:
Bioconjug Chem. 2010 July 21; 21(7): 1216–1224. doi:10.1021/bc1000033.

Well-defined, size-tunable, multi-functional micelles for efficient paclitaxel delivery for cancer treatment

Juntao Luo[†,*], **Kai Xiao**[†], **Yuanpei Li**[†], **Joyce S. Lee**[†], **Lifang Shi**[‡], **Yih-Horng Tan**[‡], **Li Xing**[§], **R. Holland Cheng**[§], **Gang-Yu Liu**[‡], and **Kit S. Lam**[†,*]

Juntao Luo: juntao.luo@ucdmc.ucdavis.edu; Kit S. Lam: kit.lam@ucdmc.ucdavis.edu

[†] Division of Hematology & Oncology, University of California, Davis Cancer Center, Sacramento, CA, 95817, USA

[‡] Department of Chemistry, University of California Davis, Davis, CA 95616, USA

[§] Department of Molecular and Cellular Biology, University of California Davis, Davis, CA 95616, USA

Abstract

We have developed a well-defined and biocompatible amphiphilic telodendrimer system (PEG-b-dendritic oligo-cholic acid) which can self-assemble into multifunctional micelles in aqueous solution for efficient delivery of hydrophobic drugs such as paclitaxel. In this telodendrimer system, cholic acid is essential for the formation of stable micelles with high drug loading capacity, owing to its facial amphiphilicity. A series of telodendrimers with variable length of PEG chain and number of cholic acid in the dendritic blocks were synthesized. The structure and molecular weight of each of these telodendrimers were characterized, and their critical micellization concentration (CMC), drug-loading properties, particle sizes and cytotoxicity were examined and evaluated for further optimization for anticancer drug delivery. The sizes of the micelles, with and without paclitaxel loading, could be tuned from 11.5 to 21 nm and from 15 to 141 nm, respectively. Optical imaging studies in xenograft models demonstrated preferential uptakes of the smaller paclitaxel-loaded micelles (17–60 nm) by the tumor, and the larger micelles (150 nm) by the liver and lung. The toxicity and anti-tumor efficacy profiles of these paclitaxel-loaded micelles in xenograft models were found to be superior to those of Taxol® and Abraxane®.

Introduction

Abraxane® and Doxil® are the first two FDA-approved nanotherapeutic agents for cancer treatment. These two agents are not likely to be able to penetrate deeply into a tumor mass due to the relatively large sizes (130 nm and 150 nm, respectively). (1–3) In order to take the full advantage of the enhanced permeability and retention (EPR) effect (4,5) for the tumor-targeting drug delivery and to ensure the deep tumor penetration, the size of the nanocarriers ought to be smaller. The optimal therapeutic nanocarriers should have the following properties (6–8): high drug loading capacity, narrow polydispersity, well-defined structure and multifunctionality, good physical and chemical stability, biocompatibility, and biodegradability. Polymeric micelles with small particle size (20–100 nm) have shown great promise as nanocarriers for efficient drug delivery.(9–11) It has been reported that the size

[*]Corresponding authors: Juntao Luo, Ph.D. Fax: (+01)916-734-6415; Prof. Kit S. Lam, M.D., Ph.D. Fax: (+01)916-734-7946.

Supporting Information Available. The experimental details of AFM studies, structures of telodendrimers, drug release and stability of the PTX loaded micelles and the duplicated *in vitro* imaging for the size effects. This material is available free of charge via the Internet at http://pubs.acs.org.

of the blank polymeric micelles can be tuned by adjusting the ratio of the hydrophobic and hydrophilic segments in the di-block copolymers.(12) In some of these micelle systems, the particle size varies relatively to the preparing conditions, such as the initial polymers concentration in the organic solvent prior to the dilution in aqueous solution (12,13), making it difficult to control in a clinical setting. The random chain propagation, chain transfer and chain termination reactions in polymerizations, especially for radical polymerization, often lead to polydispersed polymer chains.(14) Therefore, it is difficult to prepare polymeric materials, with precise structures and possessing orthogonal functional groups at specific sites, for the generation of well-defined multi-functional nanocarriers displaying targeting ligands, fluorescent probes or radionuclides.

Linear-dendritic copolymer has a well-defined and engineerable dendritic block structure at one or both ends of a linear polymer chain.(15,16) There are a few examples in the literature that hydrophobic molecules were introduced to the periphery of the dendritic segments of PEG-dendritic copolymers, generating amphiphilic linear-dendritic copolymers that could form micelles in aqueous solution. (17–20) However, the application of these linear-dendritic copolymers in drug delivery has been rarely reported. (21,22) It is probably due to the lack of suitable building blocks to form the copolymers with superior properties. Cholic acid is one of the major bile acids produced in the human liver. Its unique facial amphiphilicity makes it a very useful building block for synthesizing biocompatible polymers for drug delivery.(23) Linear cholic acid-PEG conjugate (CA-PEG) (24) and star-shaped cholic acid-centered PEG conjugate ($CA\text{-}PEG_4$) (25) have been reported to aggregate in water and form micelles. However, the drug loading capacities of these micelles are very limited. Oligomers of CA have been employed as functional molecular containers for caging hydrophobic molecules; (26–28) however, their application in drug delivery is very limited mainly due to the small and unstable cavities, and their poor water solubility. To develop a cancer therapeutic nanocarriers with optimal properties, we have designed and synthesized a new linear-dendritic block copolymer (named as telodendrimer) using three biocompatible building blocks: polyethylene glycol (PEG), L-lysine, and cholic acid (CA).

Paclitaxel (PTX) is one of the most effective anti-cancer drugs for the treatment of a wide spectrum of cancers. However, it has very poor solubility in water (1 μg/mL). The commercially available paclitaxel (Taxol®) is formulated in an oily solution (Cremophor EL/absolute ethanol, 1:1 v/v), which has been associated with severe hypersensitivity reactions. Therefore, premedications with acetaminiophen, steroid and histamine blockers are almost always required prior to PTX administration.(29). Several polymeric micelle systems have been developed for PTX delivery, but many of them had low drug loading capacity and poor stability. (30,31) Although Me-PEG-b-PDLLA micelles had shown an impressive PTX loading level of 25% w/w, they are stable for only 24 hours.(32) We have recently reported(33) the design and synthesis of a telodendrimer, $PEG^{5k}CA_8$, with a dendritic oligomer of cholic acid conjugated on one end of linear PEG, that forms a stable micelle in water and can load paclitaxel (PTX) as high as 36.5% of drug/polymer ratio (w/w). The *in vivo* antitumor efficacy of our PTX loaded $PEG^{5k}CA_8$ micelles (33) were tested in both the subcutaneous and intraperitoneal ovarian cancer mouse models and it exhibited superior toxicity profile and antitumor effects, compared with the clinical formulations of PTX, such as Taxol® and Abraxane®.

One major advantage of this telodendrimer system is the easily engineered and well defined structures, which lead to its tunable properties. In this report, we describe the design and synthesis of a series of related telodendrimers so that we can better define the relation between the structures of the telodendrimers and their physico-chemical properties for drug delivery. By varying the PEG chain length and the number of cholic acid in the dendritic

core, we were able to prepare a series of stable micelle systems with tunable particle sizes that have superior PTX loading capacities. The structure, micelle formation, drug loading properties and *in vitro* cytotoxicity of the telodendrimers were characterized. The size effects of the nanoparticles on their *in vivo* biodistribution in the xenograft model were also studied. Different from our previous study (33), we were able to achieve complete cure in the group of nude mice bearing small ovarian tumor xenograft implant by giving them five consecutive doses instead of three consecutive doses of PTX loaded $PEG^{5k}CA_8$ micelles.

Experiments

Materials and Instruments

Paclitaxel was purchased from AK Scientific Inc. (Mountain View, CA). Monomethyl terminated polyethylene glycol mono amine (MeO-PEG-NH_2, Mw =2, 3, 5 and 10 kDa, respectively) were purchased from Rapp Polymere (Tübingen, Germany). (Fmoc)lysine(Fmoc)OH was purchased from NeoMPS INC (San Diego, CA, USA), Cholic acid, Cholesterol chloroformate, lithocholic acid, heptadecanoic acid, Cremphor EL, and MTT [3-(4, 5-dimethyldiazol-2-yl)-2, 5 diphenyl tetrazolium bromid] were purchased from Sigma-Aldrich. Hydrophobic near infrared fluorescence (NIRF) dye DiD (1,1′-dioctadecyl-3,3,3′,3′-tetramethylindodicarbocyanine perchlorate, D-307) was purchased from Invitrogen. Taxol® (Mayne Pharma, Paramus, NJ) and Abraxane® (Abraxis Bioscience, LA, CA) were obtained from a hospital pharmacy. The proton NMR spectra were collected on a Bruck Avance 500 spectrometer. The mass spectra of the telodendrimer were collected on ABI 4700 MALDI TOF/TOF mass spectrometer using α-Cyano-4-hydroxycinnamic acid as a matrix. The fluorescence analysis for the critical micellization concentration (CMC) study and the colorimetric measurement in MTT assays were performed on a SpectraMaX M2 (Molecular Devices) microplate reader. The sizes of the micelles were analyzed on a zetatrac DLS particle sizer (Macrotrac).

Synthesis of telodendrimer

The telodendrimers were synthesized via solution phase condensation reactions from MeO-PEG-NH_2 with a certain molecular weight. Typical procedure for synthesis of PEG^{5k}-CA_8: (Fmoc)lysine(Fmoc)-OH (2 equ.) was coupled onto the N terminal of PEG using diisopropyl carbodimide (DIC, 2 equ.) and N-Hydroxybenzotriazole (HOBt, 2 equ.) as coupling reagents in DMF for over night. The completion of the coupling was monitored by Kaiser test: yellow color indicates no amino group left, blue color indicates the presence of amino groups. PEGylated molecules were precipitated by adding ice-cold ether and washed with ice-cold ether twice. Fmoc groups were removed by the treatment with 20% piperidine in DMF, and the PEGylated molecules were precipitated and washed three times by cold ether. White powder precipitate was dried under vacuum and another two repeat coupling of (Fmoc)lysine(Fmoc)-OH were carried out to generate a third generation of dendritic polylysine on one end of PEG. Cholic acid NHS ester, prepared according to the literature(34), was coupled to the terminal end of dendritic polylysine, resulting in PEG^{5k}-CA_8. The telodendrimer was precipitated and washed by cold ether and dissolved in water. The telodendrimer solution was filtered and then dialyzed against 4L water in a dialysis tube with MWCO of 3.5 KDa; reservoir water was refreshed completely four times in 24 h. Finally, the telodendrimer was lyophilized.

Typical synthesis of the multifunctional telodendrimer N_3-PEG^{5k}-(BocNH)-CA_8: 3-azidopropylamine (2 eq.), prepared following the procedure in the literature,(35) was coupled onto a carboxylic group of the FmocNH-PEG-COOH (5000 Dalton) using HOBt (2 eq.)/DIC (2 eq.) as coupling agents in DMF overnight, then the polymer was precipitated and washed with cold ether. After removal of the Fmoc with the treatment of 20% piperidine

solution in DMF, (Fmoc)Lys(Boc)-OH (2 eq.) was coupled onto the N terminal of PEG using DIC and HOBt as coupling reagents until a negative Kaiser test result was obtained, indicating completion of the coupling reaction. The PEGylated compounds were then precipitated and washed with cold ether. The dendritic structure of lysine was achieved by the three repeated coupling of (Fmoc)Lys(Fmoc)-OH following the above Fmoc peptide synthesis procedure. After removal of Fmoc group, cholic acid NHS ester (34) (16 eq.) was used to react with the amino groups on the third generation of dendritic polylysine to generate N_3-PEG^{5k}-(BocNH)-CA_8. This telodendrimer was subsequently dialyzed and lyophilized to yield a white powder.

Loading of paclitaxel and fluorescence dye into micelles

Paclitaxel (6 mg) and telodendrimer (20 mg) were first dissolved in chloroform (4 mL) in a 10 mL-flask. The organic solvent was rotavaporated under vacuum to form a thin film, which was further dried under high vacuum for 30 min to remove residual organic solvents. PBS buffer solution (1 mL) was added into the flask, followed by the sonication for 2 hours to disperse the polymer-drug conjugates into water. Finally, the micelle solution was filtered through a 0.22 μm filter to remove bacteria prior to *in vitro* and *in vivo* studies. The co-loading of paclitaxel with the hydrophobic near infrared dye, DiD, was following the same procedure above. In order to encapsulate same concentration of DiD into micelles with different sizes, 1 mg of DiD (a hydrophobic near infra-red (NIR) cyanine dye) and PTX (4 mg, 4 mg and 3 mg, respectively) were co-loaded into 20 mg of PEG^{2k}-CA_4, PEG^{5k}-CA_8 and PEG^{3k}-CA_4, respectively, and dispersed in 1 mL PBS solution. The loading of the PTX in micelles is measured by HPLC: 10 μL aqueous solution of the PTX loaded micelle was diluted with 90 μL of DMSO to break the micelle prior to the injection into HPLC, equipped with a UV-Vis detector. The gradient eluting solution, composed of water (A) and acetonitrile (B), was used: 1–7 min (A to B); 7–9 min (B); 9–9.5 min (B to A); 9.5–13 min (A). The column was Xterra® MS C18 5 μm, 46×150 mm column.

CMC measurement

A series concentration of the telodendrimers in PBS (100 μL) were prepared in a 96-well plate in a range from 1μg/mL to 5mg/mL. 1 μL of a stock solution of the pyrene in methanol was added into the micelle solution to make a final concentration of pyrene of 2 μM. The solution was mildly shaken for equilibrium for 2 hours. Then the fluorescence emissions of the pyrene at 391 nm were collected, respectively, at the excitation of 332 nm and 336 nm. The ratio of the intensity at 336 nm to 332 nm were plotted vs. the concentration of the telodendrimers, as reported in the literature, (36) to calculate the CMC. The CMC is determined from the threshold concentration, where the intensity ratio I336/I332 begins to increase markedly.

Drug release

The *in vitro* paclitaxel release profile was studied by dialysis technique. Aliquots of the paclitaxel-loaded micelle solution (3 mL, with a PTX concentration of 2 mg/mL) were injected into a dialysis cartridge (Pierce Chemical Inc.) with a 3.5 KDa MWCO. The cartridge was dialyzed against 1 L of PBS media under different conditions: (a) The PBS media was kept unchanged; (b) PBS media was refreshed at each time point for sampling; (c) PBS media was kept unchanged with 10 g/L of BSA and (d) PBS media was kept unchanged with 10 g/L of charcoal. The dialysis was kept at 37°C and swirled at 100 rpm. The concentration of paclitaxel remained in the dialysis cartridge at various time points was measured by HPLC. Values were reported as the means for each triplicate samples.

MTT Assay

MTT growth inhibition method was performed briefly as follow: cells were seeded in 96-well plates 24 h before treatment at a density of 3000 cells/well. After 72 h of incubation with different concentrations of telodendrimers and various formulations of paclitaxel in a humidified 37°C, 5% CO_2 incubator, MTT was added to each well at a final concentration of 0.5 mg/mL and further incubated for 4 h at 37°C. To stop the reaction, the MTT medium was removed and a 100 μL of detergent mixture (0.04 N HCl in absolute isopropanol) was added and incubated for 30 min at room temperature. The absorbance at 570 nm and 660 nm were detected using a microplate ELISA reader (SpectraMax M2, Molecular Devices, USA). Results were displayed as the cell viability [(ODtreat–ODblank)/(ODcontrol–ODblank)×100%] by three independent experiments. The IC50 value was calculated as the concentration of agents that inhibited the growth of cells by 50%.

Xenograft mouse model

Female athymic nude mice (Nu/Nu strain), 6–8 weeks age, were purchased from Harlan (Livermore, CA) and kept under pathogen-free conditions according to AAALAC guidelines and were allowed to acclimatize for at least 4 days prior to any experiments. SKOV-3 ovarian cancer cells transfected with luciferase gene (7×106) in a 100 μL of mixture of PBS and Matrigel (1:1 v/v) without fetal bovine serum (FBS) were injected subcutaneously into nude mice to form subcutaneous nodules.

Fluorescence optical imaging

SKOV-3 tumor bearing mouse was injected via tail vein with the PBS solution (1% of body weight of mouse) of micelles with different sizes co-loaded with the same concentration of DiD (hydrophobic dye) together with paclitaxel. Mice were anesthetized, and optically imaged with a Kodak Image Station 2000MM at 30min to 1 h, 2 h, 4h and 24 h. At the end of the experiment, the animal was sacrificed and all the major organs and tumor were excised for *ex vivo* imaging.

Therapeutic studies

Nude mice bearing human SKOV-3 (transfected with luciferase gene) ovarian cancer tumor (50 mm^3) were treated (five mice per group) with various formulations of paclitaxel at day 0, 4, 8, 12, 16 for 5 consecutive doses. Abraxane® and Taxol® at maximum tolerated dose (MTD) of 30 mg/Kg and 15 mg/Kg, respectively, were given intravenously. PTX loaded $PEG^{5k}CA_8$ were administered at two dose levels of 15 and 45 mg/Kg, in which the latter dose is the MTD. One day after the last treatment, blood was obtained for blood counts and serum chemistries. Digital callipers were used to measure the length and width of the tumor twice a week, and the tumor sizes were calculated using the following formula: ($width^2$ × length)/2. A luciferin kinetic study was performed for each animal to determine the peak signal time. Briefly, 150 mg/Kg D-luciferin was injected intraperitoneal (i.p.), and mice were anesthetized with pentobarbital (i.p., 60 mg/Kg), the bioluminescence imaging was obtained at 15 min after luciferin injection using Kodak imaging station 2000 MM.

Results and Discussion

The chemical structure of PEG^{5k}-CA_8, a representative telodendrimer, is shown in Figure 1. According to our nomenclature, “5k” represents the molecular weight of PEG (i.e. 5000 Dalton) and “8” indicates the number of CA subunits in the telodendrimer. PEG^{5k}-CA_8 is soluble in water and self-assembles into micelles with a size of 21 ± 4 nm. More importantly, it is capable of encapsulating hydrophobic drugs such as PTX. Bi-functional FmocNH-PEG-COOH is used as the starting material to construct the multifunctional

telodendrimers (Figure 1), and the azide group is introduced at the distal C-terminal of PEG and can be conveniently used for the ligation of cell surface targeting ligands (37) or antibodies. The Boc protected amino groups adjacent to the dendritic core are reserved for the conjugation of fluorescent dyes, radionuclides, or drug molecules to the micelles, and hydrophobic drugs or probes can be physically encapsulated inside the micelles as shown in the cartoon in Figure 1.

To study the physical properties of various telodendrimers and their effects on the *in vivo* passive tumor targeting effects of the resulting nanoparticle, mono-functionalized MeO-PEG-NH_2 with different PEG chain length (2–10 kDa) were used for linking various number of CA (4, 8 and 16) to the dendritic block to prepare a series of telodendrimers (Table 1). Representative structure of the inert telodendrimer is shown in Scheme S-1 in the supporting information. The molecular weights of the telodendrimers were measured with MALDI-TOF mass spectrometry. The mono-dispersed mass traces were detected for the starting PEG and the telodendrimers. The molecular weight shifts between the telodendrimers and the corresponding starting PEG were almost identical to the mass increase by the conjugation of the oligo-cholic acids (Figure S-1 in supporting information). The molecular weights of the telodendrimers from MALDI-TOF MS (Table 1) were very similar to the theoretical value. The molecular weights of the telodendrimers were also determined by NMR spectrometry, based on the ratio of the proton signals of the three methyl groups on cholic acid (0.6–1.1 ppm) to the proton signals of the PEG (3.5–3.65 ppm) in the ^1H NMR spectra of the telodendrimers in $CDCl_3$ (Figure 4a). The molecular weights obtained from NMR method were also very close to the theoretical values (Table 1), indicating the well-defined structures of telodendrimers. These telodendrimers were prepared via the well-established stepwise Fmoc peptide chemistry. The soluble PEG-supported conjugation reactions can be driven to completion by adding excess amount of reagents. Subsequently, the PEGylated intermediate and products can be easily isolated and purified via the precipitation and washing with cold ether, thus ensuring that the structures of the telodendrimers are well-defined. As shown Figure 1, another advantage of this stepwise synthesis is that the structure of the telodendrimer can be easily engineered and multiple functional groups can be introduced into the polymer at particular density and at the specific sites.

The critical micelle concentration (CMC) of the telodendrimers was measured with a standard fluorescence technique using pyrene as the probe.(36) As shown in Figure 2, the CMCs of the telodendrimers with different PEG chain length and the number of the cholic acid vary from 8 μg/mL to 250 μg/mL, corresponding to 0.97 μM to 67 μM (Table 1), due to the changes of the amphiphilicity. We found that the telodendrimers with larger number of cholic acids, such as PEG^{2k}-CA_8 and PEG^{10k}-CA_{16}, had low CMCs around 1 μM and yielded larger micelles with a heterogeneous size distribution. After loaded with PTX, significant precipitation was observed. Very low or undetectable PTX loading were observed after the removal of precipitates (Table 1). Micelles prepared from telodendrimers with medium CMC values (5–7.9 μM), such as PEG^{2k}-CA_4, PEG^{3k}-CA_8 and PEG^{5k}-CA_8, were found to be very stable and homogeneous in size before and after PTX loading. Those telodendrimers composed of fewer cholic acid molecules (PEG^{3k}-CA_4 and PEG^{5k}-CA_4) and with high CMCs (12.5 and 67 μM, respectively) were found to be able to form smaller micelles (10 and 15 nm, respectively) prior to drug loading. After PTX loading, the micelles increased in size up to 131 nm and 141 nm, respectively at relatively low PTX loading level, however, remaining very stable and homogeneous in size. While more PTX was added (>10% w/w drug/polymer), significant precipitation occurred for PEG^{5k}-CA_4.

Most of telodendrimers discussed above, except PEG^{2k}-CA_8 and PEG^{10k}-CA_{16}, can be readily dissolved in water at concentration up to 200 mg/mL. In the micelle characterization, PTX loading and *in vivo* xenograft studies, we decided to keep the concentration of the

telodendrimers at 20 mg/mL, which provided effective PTX concentration and exhibited the low viscosity needed for tail vein injection of the nanotherapeutics in the *in vivo* animal experiments. Through adjusting the PEG chain length and the number of CA subunits in the telodendrimers, the particle sizes of the PTX loaded micelles can be tuned ranging from 15 nm to 141 nm. Among them, PEG^{5k}-CA_8 has a medium particle size of 61 nm and the highest PTX loading capacity (7.3 mg PTX loaded in 20 mg PEG^{5k}-CA_8/mL), which is equivalent to 36.5% (w/w) of drug/polymer ratio (Figure 3a). The final particle size of PTX-loaded PEG^{5k}-CA_8 (with CMC around 5 μM) showed a modertate increase in size, while other telodendrimers, such as PEG^{3k}-CA_4 (CMC at 12.5 μM), produced a significant size increase at high drug loading level (Figure 3b). Our telodendrimer micelle systems can also effectively deliver other therapeutic agents including etoposide, a topoisomerase II inhibitor for cancer treatment, at an etopside/polymer ratio of 18.5% in PEG^{5k}-CA_8 (Figure 3d). By increasing the amount of drug added, the etoposide-loaded micelles exhibited very similar changes in sizes when combining with different telodendrimer micelles: PEG^{3k}-CA_8 and PEG^{5k}-CA_8 maintain their small particle sizes with high drug loading capacities, while and the size of etopside-PEG^{3k}-CA_4 micelles increases dramatically with the increased drug loading (Figure 3c).

We have also substituted cholic acid in PEG^{5k}-CA_8 with other natural lipophilic molecules such as cholesterol formate (CF), lithocholic acid (LA) (both with planar steroid scaffold), and heptadecanoic acid (HA) (linear fatty acid). The resulting telodendrimers, with low CMCs at approximately 1 μM, tend to form precipitate in aqueous solution and their PTX loading capacities are rather low (Table 1). The above studies indicate that cholic acid is essential to form stable telodendrimer micelles. Presumably, under aqueous environment, the facial amphiphilic cholic acids in the dendritic core can arrange their hydrophobic convex surfaces to the interior of micelle, and place the opposite hydrophilic surfaces against the aqueous environment to lower the energy, and together with PEG to stabilize the hydrophobic components inside the micelles. Additionally, some of the cholic acids might be randomly packed inside the hydrophobic core and their hydroxyl groups may form hydrogen bonds with the hydrophilic groups in PTX; such interactions may contribute to the good drug loading capacity of these micelles.(38)

^{1}H NMR spectra of PEG^{5k}-CA_8 in $CDCl_3$ revealed the expected structure of the telodendrimer. However, when the ^{1}H NMR spectrum was collected in deuterated water, the cholane signals (0.6–2.2 ppm) were greatly suppressed (Figure 4a), indicating that the dendritic oligo-CA was tightly packed in the core of the micelles with high microviscosity. The similar phenomena were also reported in other micelles systems. (32, 36, 39) In the cryoTEM study (Figure 4b), PTX was loaded into PEG^{5k}-CA_8 micelles (7.3 mg PTX/mL) in order to increase the density of the core and enhance the contrast against the background. Spherical micelles were observed with *in situ* sizes ranging from 30 to 60 nm calibrated with tobacco mosaic virus (18 nm in width), which is consistent with the DLS measurement (61 ± 21 nm, Table 1). Blank micelles (16 ± 4 nm by DLS) and PTX-loaded micelles (6.4 mg PTX/mL, 23 ± 8 nm by DLS) prepared from thiol-functionalized HS-PEG^{5k}-CA_8 (Scheme S-2 in the supporting information) were immobilized on gold surfaces for atomic force microscopy (AFM) scanning. Tapping mode AFM topographs were obtained in aqueous solution. Both the empty and drug-loaded micelles appeared as individually immobilized nanoparticles with average sizes of 15 nm and 26 nm, respectively (Figure 4c-f), which were close to the particle sizes obtained by DLS measurement.

The morphology of the aggregates formed by other telodendrimers was studied by TEM. As mentioned above, PEG^{3k}-CA_4 and PEG^{5k}-CA_4 when loaded with hydrophobic molecules such as PTX, tend to form large nanoparticles. Interestingly, rod shape aggregates (40 nm in width and several hundreds nm in length) were observed under TEM imaging of the PTX-

PEG^{5k}-CA_4 sample (Figure 5a). $PEG^{2k}CA_4$, on the other hand, was observed to form gel or gel particles at high concentration (30 mg/mL) upon storage. After loaded with hydrophobic payloads, such as NIR dye (DiD) or PTX, the micelle solution became more viscous upon storage overnight at room temperature. Spherical micelles (15 nm) and nano-fibers (about 2 nm thickness) were observed under CryoTEM (Figure 5b). This indicates that the morphology could change from the spherical micelles (low viscosity) to fibers (high viscosity) during storage. The morphological outcome is probably determined by the structure as well as the amphiphilic balance of the telodendrimers. The packing parameters (ratio of hydrophobic/hydrophilic blocks) have been widely used to predict the morphology of the micelles formed by linear amphiphilic copolymers.(40, 41) However, the same rule may not apply to our telodendrimers with facial amphiphilicity and bulky cluster of cholic acids, Work is currently underway in our laboratory to study the relationship between the packing parameters and morphological outcome of the telodendrimer-based micelles.

The stability of the PTX loaded PEG^{5k}-CA_8 micelles were followed by the DLS particle sizer. The particle size of these PTX-loaded micelles in aqueous solution was found to be highly stable at 4°C for over 6 months, no further aggregations and no needle crystals of PTX were observed. In contrast, most of the PTX-loaded polymeric micelles reported in the literature are lack of stability (from a few hours to days). (30–32) Even Abraxane®, the FDA-approved albumin nanoparticle-bound PTX, tends to precipitate 24 hours after reconstituted with saline (Supporting information, Figure S-2). Upon dilution with PBS to 125 fold to mimic the dilution by the blood pool through intravenous (iv) injection, needle-like crystals of PTX were observed in the diluted Taxol® (Cremophor formulation of PTX) solution within a month. In contrast, this was not observed in the diluted PTX loaded PEG^{5k}-CA_8 micelle solutions even for 12 months, indicating that the PTX complex inside these micelles is very stable.

Upon dialysis in a cassette (MWCO 3500 Dalton) against PBS with different sink conditions over time, PTX can diffuse out from the micelle systems, but no burst release was observed (Figure 6). Under the condition of frequently refreshed PBS during sampling, the drug release was much faster than that in the unchanged PBS. The condition with charcoal in the PBS reservoir (without changing PBS) allowed efficient absorption of the released PTX, which mimic the *in vivo* protein binding and cellular uptake of drug, the drug release was even more faster than that in the refreshed PBS. Bovine serum albumin (BSA) was found to be not efficient to absorb the released free PTX, resulting in slow drug release rate, which is very similar to that in the unchanged PBS condition. In addition, PTX needle crystals were observed in the dialysate in the unchanged PBS and in BSA solution conditions, which lead to some variations in the measurements. However, the needle crystals were not found in the dialysates in the conditions of refreshed PBS and in the unchanged PBS with charcoal. Approximately 50% of the loaded PTX was released from the micelles after 24 hours in the sink conditions, and no burst release was observed during the fist few hours. Interestingly, we found that the PTX release rate of the samples, which had been prepared and stored for two months, were lower compared to the freshly loaded samples and the release pattern was in a linear mode (Supporting information, Figure S-3). One possible explanation for this observation is the crystallization of PTX inside the core of the micelle or the crystallization of hydrophobic segments of the telodendrimer over time. To address this question, X-ray diffraction (XRD) studies were performed on these samples. Distinct PEG crystalline peaks were identified at 19.1° and 23.3° (42,43) (Supporting information, Figure S-4); however, no crystalline peaks for PTX (42) or hydrophobic moieties (Cholic acid) were detected in the XRD spectra. Instead, the typical diffraction curve of the amorphous polymer was observed from 10° to 30°, indicating that the micellar core loaded with PTX was amorphous. The XRD studies of these old samples indicate the slow PTX release was not caused by the crystallization of PTX or the hydrophobic segments inside the micelles. The DSC

(differential scanning colorimetry) analysis revealed an increased Tg (glass transition temperature, 200°C) of the cholane core for a PTX-PEG^{5k}CA$_8$ sample lyophilized after storage for 55 days at 4°C, compared with the same sample lyophilized at earlier time point, such as day 5 (Tg: 179 °C) (Supporting information, Figure S-5). Thus, the slow PTX release from the old PTX-loaded samples may be due to the more compact core structures formed by the rearrangement of the dendritic cholane segments during storage.

The cytotoxicity of the telodendrimers in cell culture was evaluated via the MTT assays. As shown in Figure 7a, up to 1 mg/mL of PEG^{5k}CA$_8$ in the cell culture media, no significant cytotoxicity was observed on MDA-MB-231 breast cancer cells (IC50: 1.5 mg/mL). However, the telodendrimers with shorter PEG chain length (2 and 3 KDa) exhibited cytotoxic effects at relatively lower concentrations, and the IC50 of PEG^{2k}CA$_4$ PEG^{3k}CA$_4$ PEG^{3k}CA$_8$ were 45, 126 and 150 μg/mL, respectively. PEG^{5k}CA$_8$ remained to be rather non-toxic, compared to other telodendrimers with shorter PEG chains, to other cancer cell types including SKOV-3 (ovarian cancer) and HT29 (colon cancer). This may be explained by the extra stereo hindrance of the longer PEG preventing the interaction between the micelles and cells. The cell killing efficacies of PTX loaded telodendrimers, such as PEG^{5k}-CA$_8$, PEG^{3k}CA$_4$ and PEG^{3k}CA$_8$ and the two clinical formulations of PTX (Taxol® and Abraxane®) on SKOV-3 cells were found to be comparable, and the IC50 ranged from 4.3 to 6.2 ng/mL, after 72 hours of continuous incubation with the drugs (Figure 7b). The corresponding concentrations of the telodendrimers at the IC50 of PTX formulations are 20–30 ng/mL, which are far less than the IC50 of the blank telodendrimers (45–1500 μg/mL), indicating the potential clinical applications of these telodendrimers for delivery of PTX. The IC50 of PTX and PTX loaded PEG^{5k}CA$_8$ on the MDA-MB-231 cells, were observed to be higher than that in SKOV3 cells at 45 ng/mL and 17 ng/mL, respectively, over 72 hours of continuous drug exposure.

To study the effects of particle size on the *in vivo* biodistribution of nanoparticles, DiD (a hydrophobic near infra-red (NIR) cyanine dye, 1 mg/mL) was co-loaded with PTX (4 mg/mL, 4 mg/mL and 3 mg/mL, respectively) into 20 mg/mL micelle solutions of PEG^{2k}-CA$_4$, PEG^{5k}-CA$_8$ and PEG^{3k}-CA$_4$, to form three fluorescence labeled micelle preparations with distinct sizes of 17 nm, 64 nm and 154 nm, respectively (Figure 8a). Each of these three sizes of DiD-loaded micelles was incubated with Raw 264.7 macrophage cells for 2 h. The cells were then washed three times with PBS, fixed with 70% ethanol and observed under confocal fluorescence microscope. As shown in Figure 8b, the larger micelles (154 nm), compared to the two smaller ones, were preferentially taken up by the macrophages, which was subsequently confirmed by the flow cytometry analysis (data were not shown). NIR fluorescent imaging was used to evaluate the *in vivo* biodistribution of the three micelles with different sizes in nude mice bearing the SKOV-3 ovarian cancer xenografts (subcutaneous implants). The mice were injected via the tail vein with the same volume of the above three PTX-DiD loaded micelle preparations in PBS. *Ex vivo* imaging of the excised organs and tumors were performed at 24 h after injection. As shown in Figure 8c, the larger nanoparticles (154 nm) clearly exhibited the highest fluorescence intensity in the liver and the lungs, likely due to nonspecific uptake by macrophages in those organs; moreover, the fluorescent uptake by the tumor was very low. In contrast, tumor uptake of the smaller micelles (17 and 64 nm) was much higher than normal organs. The duplicated images in a different set of mice showed similar size effects on the biodistributions (Figure S-6 in supporting information). The *in vivo* NIR images of a tumor bearing mouse treated with the DiD-PTX-PEG^{5k}CA$_8$ was recorded over time (Figure 8d). It is evident that the accumulation of the DiD loaded micelles at the tumor site via the EPR effect began at 2 h after injection, and continued to increase over the next 24 h period. In contrast, tumor targeting was not found in the tumor-bearing mice treated with the free dye.(33) Consistent with imaging study of the size effect, PTX-loaded PEG^{5k}-CA$_8$ have been shown to be

superior to Abraxane® and Taxol® in the treatment of both subcutaneous and intraporitoneal xenograft ovarian cancer murine models.(33) We believe PTX-PEG^{2k}-CA$_4$, with smaller micelle sizes (17 nm), will be able to penetrate more deeply into the solid tumor and potentially result in better antitumor effects in tumor xenograft models. This study is currently undergoing in our laboratory.

In our previous report (33), we were able to demonstrate that PTX-loaded PEG^{5k}-CA$_8$ (3 consecutive doses every 4 days) slowed down the growth of ovarian cancer xenograft (100–200 mm^3) considerably however, the tumors eventually progressed and complete cure was never achieved. In this study, we treated 5 groups of mice with 5 consecutive doses of drugs given i.v. every 4 days when the xeongraft implants reached 50 mm^3 in size. As expected, rapid tumor growth was observed beginning on day 16 in the control group treated with PBS (Figure 9). In contrast, no tumor growth was detected in mice treated with each of these five PTX regimens until day 35 when the tumors began to grow in the Taxol® group at 15 mg/kg (MTD dosage for five consecutive treatment(44)). By day 40, tumor growth also began in the Abraxane group at 30 mg/kg (MTD dosage for five consecutive treatment(44)) and the low dose PEG^{5k}-CA$_8$ (15 mg/kg) group. For the high dose PEG^{5k}-CA$_8$ group at 45 mg/kg (MTD dosage for five consecutive treatment), the luciferase signal was undetectable by day 42 (supporting information Figure S-7) and there was no signs of palpable tumor over 3 months, which indicated that there was no residual disease and complete cure was achieved. Unlike Taxol®and Abraxane®, myelosuppression from the PTX-loaded PEG^{5k}-CA$_8$ was minimal (supporting information Figure S-8). No weight loss was observed in mice treated with these new nanoformulations (supporting information Figure S-9), while consistent weight loss was observed in those treated with Taxol®.

In summary, we have developed a well defined, engineerable and multifunctional telodendrimer system, which can self-assemble to form micelles in aqueous condition. By optimizing the structures of the telodendrimers, biocompatible nanocarriers have been obtained with tunable sizes and efficient PTX and etoposide loading properties. We have found that the size of the micelles can greatly influence their *in vivo* biodistribution. The smaller drug loaded micelles (17 nm and 64 nm) were more readily and efficiently to carry the loaded hydrophobic anticancer drugs to the tumor sites via EPR effects. In contrast, micelles with larger sizes (154 nm) were found to have very high uptake in liver and lung, but low uptake in tumor. In the *in vivo* antitumor efficacy studies in nude mice bearing early stage tumor xenografts, the toxicity profile and antitumor effects for PTX-loaded PEG^{5k}-CA$_8$ were observed to be superior to those of Abraxane® and Taxol®, and the cure of the disease was achieved in the group treated with PTX-loaded PEG^{5k}-CA$_8$ at its MTD dosage.

Supplementary Material

Refer to Web version on PubMed Central for supplementary material.

Acknowledgments

The authors thank the editorial assistance provided by Mr. Joel Kugelmass and the financial support from NIH U19CA113298, R21CA128501, and RO1CA115483. We also thank Dr. Mullen and Prof. Weiss at The Pennsylvania State University for their insightful information with respect to displacement in 1-adamantanethiol SAM. This work was also supported by the Institute for Complex Adaptive Matter (ICAM) (postdoctoral fellowship to (L.S.)), the University of California at Davis (CHE 0809977) and the National Institutes of Health (R21GM77850-01).

References

1. Unezaki S, Maruyama K, Hosoda JI, Nagae I, Koyanagi Y, Nakata M, Ishida O, Iwatsuru M, Tsuchiya S. Direct measurement of the extravasation of polyethyleneglycol-coated liposomes into solid tumor tissue by *in vivo* fluorescence microscopy. Int J Pharm. 1996; 144:11–17.
2. Oku N. Anticancer therapy using glucuronate modified long-circulating liposomes. Adv Drug Deliv Rev. 1999; 40:63–73. [PubMed: 10837780]
3. Senior JH. Fate and behavior of liposomes *in vivo*: a review of controlling factors. Crit Rev Ther Drug Carrier Syst. 1987; 3:123–93. [PubMed: 3542245]
4. Maeda H. The enhanced permeability and retention (EPR) effect in tumor vasculature: the key role of tumor-selective macromolecular drug targeting. Adv Enzyme Regul. 2001; 41:189–207. [PubMed: 11384745]
5. Jain RK. Vascular and interstitial barriers to delivery of therapeutic agents in tumors. Cancer Metastasis Rev. 1990; 9:253–66. [PubMed: 2292138]
6. Cho K, Wang X, Nie S, Chen ZG, Shin DM. Therapeutic nanoparticles for drug delivery in cancer. Clin Cancer Res. 2008; 14:1310–6. [PubMed: 18316549]
7. Ferrari M. Cancer nanotechnology: opportunities and challenges. Nat Rev Cancer. 2005; 5:161–171. [PubMed: 15738981]
8. Peer D, Karp JM, Hong S, Farokhzad OC, Margalit R, Langer R. Nanocarriers as an emerging platform for cancer therapy. Nat Nanotechnol. 2007; 2:751–60. [PubMed: 18654426]
9. Trubetskoy VS. Polymeric micelles as carriers of diagnostic agents. Adv Drug Deliv Rev. 1999; 37:81–88. [PubMed: 10837728]
10. Liu J, Lee H, Allen C. Formulation of drugs in block copolymer micelles: drug loading and release. Curr Pharm Des. 2006; 12:4685–701. [PubMed: 17168772]
11. Tong R, Cheng J. Anticancer Polymeric Nanomedicines. Polymer Rev. 2007; 47:345–381.
12. Riley T, Stolnik S, Heald CR, Xiong CD, Garnett MC, Illum L, Davis SS, Purkiss SC, Barlow RJ, Gellert PR. Physicochemical Evaluation of Nanoparticles Assembled from Poly(lactic acid)-Poly(ethylene glycol) (PLA-PEG) Block Copolymers as Drug Delivery Vehicles. Langmuir. 2001; 17:3168–3174.
13. Letchford K, Liggins R, Wasan KM, Burt H. *In vitro* human plasma distribution of nanoparticulate paclitaxel is dependent on the physicochemical properties of poly(ethylene glycol)-block-poly(caprolactone) nanoparticles. Eur J Pharm Biopharm. 2009; 71:196–206. [PubMed: 18762253]
14. Hirao A, Hayashi M, Loykulnant S, Sugiyama K, Ryu SW, Haraguchi N, Matsuo A, Higashihara T. Precise syntheses of chain-multi-functionalized polymers, star-branched polymers, star-linear block polymers, densely branched polymers, and dendritic branched polymers based on iterative approach using functionalized 1,1-diphenylethylene derivatives. Prog Polym Sci. 2005; 30:111–182.
15. Chapman TM, Hillyer GL, Mahan EJ, Shaffer KA. Hydraamphiphiles: Novel Linear Dendritic Block Copolymer Surfactants. J Am Chem Soc. 1994; 116:11195–6.
16. van Hest JCM, Delnoye DAP, Baars MWPL, van Genderen MHP, Meijer EW. Polystyrene-dendrimer amphiphilic block copolymers with a generation-dependent aggregation. Science. 1995; 268:1592–5. [PubMed: 17754610]
17. Gillies ER, Jonsson TB, Frechet JM. Stimuli-responsive supramolecular assemblies of linear-dendritic copolymers. J Am Chem Soc. 2004; 126:11936–43. [PubMed: 15382929]
18. Chang Y, Kwon YC, Lee SC, Kim C. Amphiphilic Linear PEO-Dendritic Carbosilane Block Copolymers. Macromolecules. 2000; 33:4496–4500.
19. Gitsov I, Wooley KL, Hawker CJ, Ivanova PT, Frechet JMJ. Synthesis and properties of novel linear-dendritic block copolymers. Reactivity of dendritic macromolecules toward linear polymers. Macromolecules. 1993; 26:5621–7.
20. Iyer J, Fleming K, Hammond PT. Synthesis and Solution Properties of New Linear-Dendritic Diblock Copolymers. Macromolecules. 1998; 31:8757–8765.
21. Gillies ER, Frechet JM. pH-Responsive copolymer assemblies for controlled release of doxorubicin. Bioconjug Chem. 2005; 16:361–8. [PubMed: 15769090]

22. Lee CC, Gillies ER, Fox ME, Guillaudeu SJ, Frechet JM, Dy EE, Szoka FC. A single dose of doxorubicin-functionalized bow-tie dendrimer cures mice bearing C-26 colon carcinomas. Proc Natl Acad Sci U S A. 2006; 103:16649–54. [PubMed: 17075050]
23. Zhu XX, Nichifor M. Polymeric Materials Containing Bile Acids. Acc Chem Res. 2002; 35:539–546. [PubMed: 12118993]
24. Kim IS, Kim SH. Evaluation of polymeric nanoparticles composed of cholic acid and methoxy poly(ethylene glycol). Int J Pharm. 2001; 226:23–9. [PubMed: 11532566]
25. Luo J, Giguere G, Zhu XX. Asymmetric Poly(ethylene glycol) Star Polymers with a Cholic Acid Core and Their Aggregation Properties. Biomacromolecules. 2009; 10:900–906. [PubMed: 19281151]
26. Zhao Y. Facial amphiphiles in molecular recognition: From unusual aggregates to solvophobically driven foldamers. Curr Opin Colloid Interface Sci. 2007; 12:92–97.
27. Janout V, Regen SL. Bioconjugate-Based Molecular Umbrellas. Bioconjugate Chem. 2009; 20:183–192.
28. Chen Y, Luo J, Zhu XX. Fluorescence study of inclusion complexes between star-shaped cholic acid derivatives and polycyclic aromatic fluorescent probes and the size effects of host and guest molecules. J Phys Chem B. 2008; 112:3402–9. [PubMed: 18293965]
29. Weiss RB, Donehower RC, Wiernik PH, Ohnuma T, Gralla RJ, Trump DL, Baker JR Jr, Van Echo DA, Von Hoff DD, Leyland-Jones B. Hypersensitivity reactions from taxol. J Clin Oncol. 1990; 8:1263–8. [PubMed: 1972736]
30. Liggins RT, Burt HM. Polyether-polyester diblock copolymers for the preparation of paclitaxel loaded polymeric micelle formulations. Advanced Drug Delivery Reviews. 2002; 54:191–202. [PubMed: 11897145]
31. Le Garrec D, Ranger M, Leroux JC. Micelles in anticancer drug delivery. Adv Drug Deliv Rev. 2004; 2:15–42.
32. Zhang X, Jackson JK, Burt HM. Development of amphiphilic diblock copolymers as micellar carriers of taxol. Int J Pharm. 1996; 132:195–206.
33. Xiao K, Luo J, Fowler WL, Li Y, Lee JS, Xing L, Cheng RH, Wang L, Lam KS. A self-assembling nanoparticle for paclitaxel delivery in ovarian cancer. Biomaterials. 2009; 30:6006–16. [PubMed: 19660809]
34. Pandey PS, Rai R, Singh RB. Synthesis of cholic acid-based molecular receptors: head-to-head cholaphanes. J Chem Soc, Perkin Trans. 2002; 1:918–923.
35. Lampkins AJ, O'Neil EJ, Smith BD. Bio-orthogonal Phosphatidylserine Conjugates for Delivery and Imaging Applications. J Org Chem. 2008; 73:6053–6058. [PubMed: 18616222]
36. Kim C, Lee SC, Kang SW, Kwon IC, Kim YH, Jeong SY. Synthesis and the micellar characteristics of poly(ethylene oxide)-deoxycholic acid conjugates. Langmuir. 2000; 16:4792–4797.
37. Aina OH, Liu R, Sutcliffe JL, Marik J, Pan CX, Lam KS. From combinatorial chemistry to cancer-targeting peptides. Mol Pharm. 2007; 4:631–51. [PubMed: 17880166]
38. Lee J, Cho EC, Cho K. Incorporation and release behavior of hydrophobic drug in functionalized poly(D, L-lactide)-block-poly(ethylene oxide) micelles. J Control Release. 2004; 94:323–35. [PubMed: 14744484]
39. Weimer MW, Scherman OA, Sogah DY. Multifunctional Initiators Containing Orthogonal Sites. One-Pot, One-Step Block Copolymerization by Simultaneous Free Radical and Either Cationic Ring-Opening or Anionic Ring-Opening Polymerization. Macromolecules. 1998; 31:8425–8428.
40. Antonietti M, Foerster S. Vesicles and liposomes: A self-assembly principle beyond lipids. Adv Mater. 2003; 15:1323–1333.
41. Christian DA, Cai S, Bowen DM, Kim Y, Pajerowski JD, Discher DE. Polymersome carriers: From self-assembly to siRNA and protein therapeutics. Eur J Pharm Biopharm. 2009; 71:463–474. [PubMed: 18977437]
42. Guo XD, Tan JP, Kim SH, Zhang LJ, Zhang Y, Hedrick JL, Yang YY, Qian Y. Computational studies on self-assembled paclitaxel structures: templates for hierarchical block copolymer assemblies and sustained drug release. Biomaterials. 2009; 30:6556–63. [PubMed: 19717188]

43. Kang N, Perron ME, Prud'homme RE, Zhang Y, Gaucher G, Leroux JC. Stereocomplex block copolymer micelles: core-shell nanostructures with enhanced stability. Nano Lett. 2005; 5:315–9. [PubMed: 15794618]

44. Desai N, Trieu V, Yao Z, Louie L, Ci S, Yang A, Tao C, De T, Beals B, Dykes D, Noker P, Yao R, Labao E, Hawkins M, Soon-Shiong P. Increased antitumor activity, intratumor paclitaxel concentrations, and endothelial cell transport of cremophor-free, albumin-bound paclitaxel, ABI-007, compared with cremophor-based paclitaxel. Clin Cancer Res. 2006; 12:1317–24. [PubMed: 16489089]

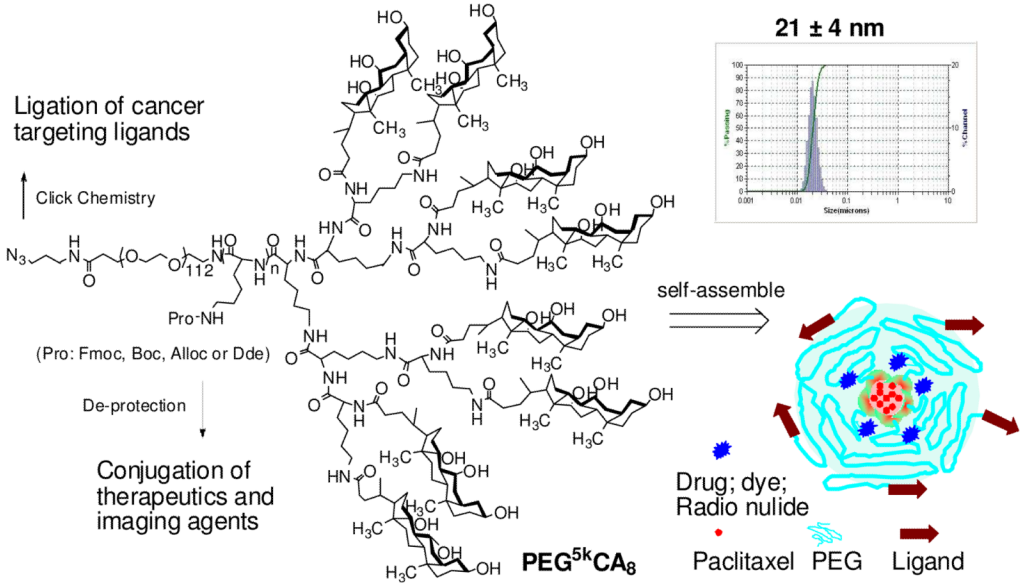

Figure 1.

The chemical structure of PEG^{5k}-CA_8 with multiple functional groups and its size measured by DLS particle sizer, the cartoon illustrates the functionalized micelles formed by telodendrimers.

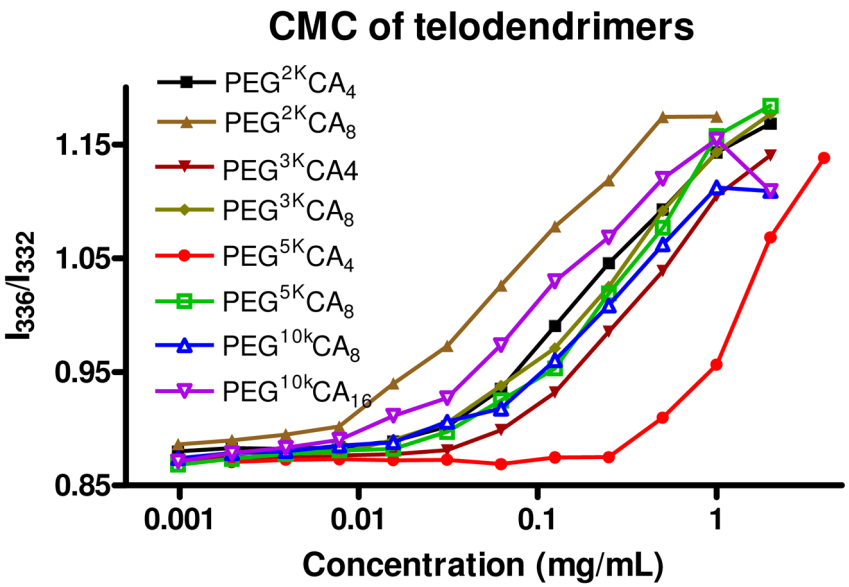

Figure 2.

The CMC studies of the telodendrimers via fluorescence technique using pyrene as a probe molecule. The emissions of pyrene at 391 nm were collected through the excitation at 332 nm and 336 nm, respectively. The ratios of I_{336}/I_{332} are plotted vs the concentration of the telodendrimers. [pyrene] is 2E-6 M and the data were the averages of triplicated measurements.

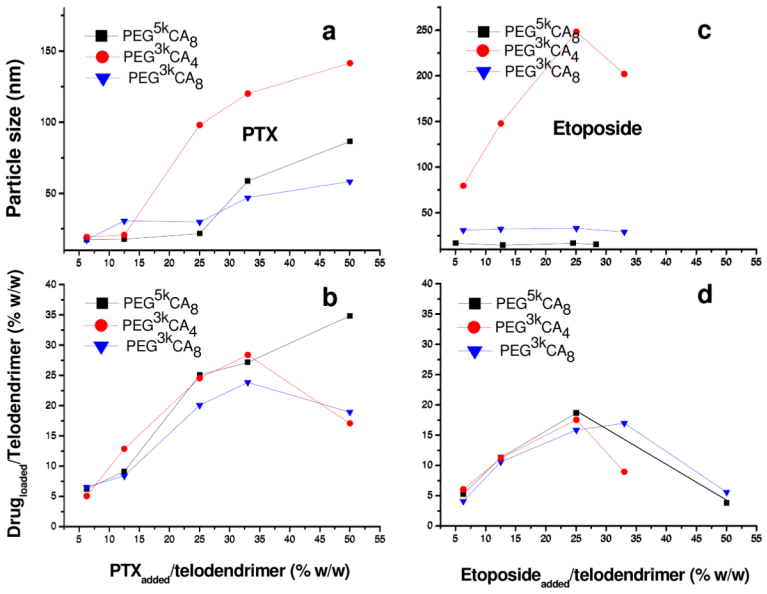

Figure 3.

The relationships of the particle size of the PTX and etoposide loaded micelles formed by different telodendrimers (a, c) and the drug/telodendrimer ratios in drug loaded micelles (b, d) vs. the feed ratios of drug/telodendrimers during the drug loading, respectively. The concentrations of telodendrimers were 20 mg/mL.

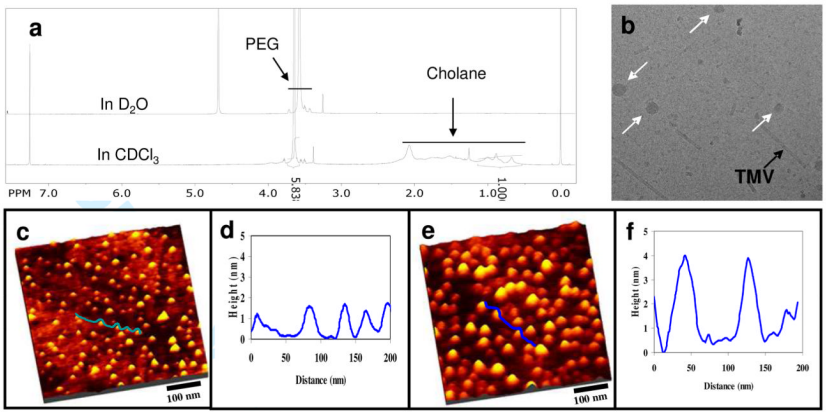

Figure 4.

(a) ^{1}H NMR spectra of PEG^{5k}-CA_8 were recorded in $CDCl_3$ and D_2O, the suppression of cholic acid signals in D_2O indicates the entanglement of cholanes in water by the formation of micelles; (b) CryoTEM images of PEG^{5k}-CA_8 loaded with PTX in the presence of tobacco mosaic virus (TMV) as calibration standard (18 nm in width); tapping mode AFM topographs of (c) the HS-PEG^{5K}-CA_8 micelles and (e) PTX loaded HS-PEG^{5K}-CA_8 micelles on gold surfaces, and the corresponding cursor profiles are represented in (d) and (f), respectively, to review the 3D sizes.

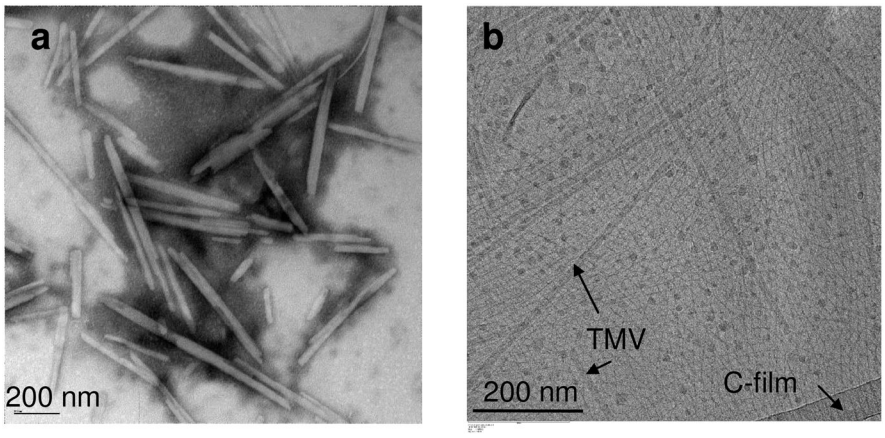

Figure 5.
(a) TEM images of the PTX loaded PEG^{5k}-CA_4 (20% w/w) solutions. The rod-like aggregates were observed with 40 nm in width and several hundreds nm in length (b) CryoTEM images of DiD loaded PEG^{2k}-CA_4 in the presence of tobacco mosaic virus (TMV) as calibration standard (18 nm in width); the spherical micelles (15 nm) and thin nanofibers (2 nm in thickness) were observed.

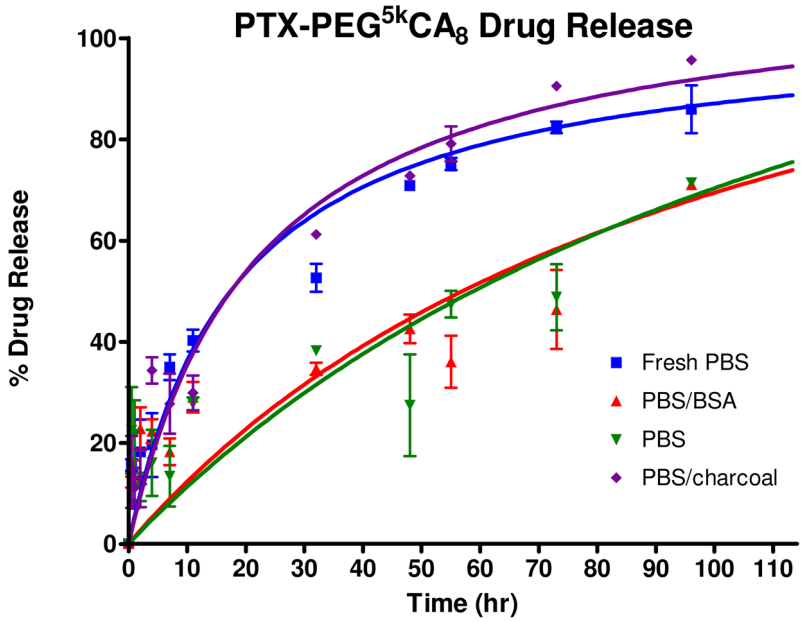

Figure 6.

The accumulative paclitaxel released from micelles formed by PEG^{5k}-CA_8 in PBS (pH 7.4) at 37°C with different sink conditions: unchanged PBS; refreshed PBS, unchanged PBS with 10 mg/mL of BSA and charcoal, respectively. The concentrations of PTX were 2 mg/mL. The data points were the average of three measurements.

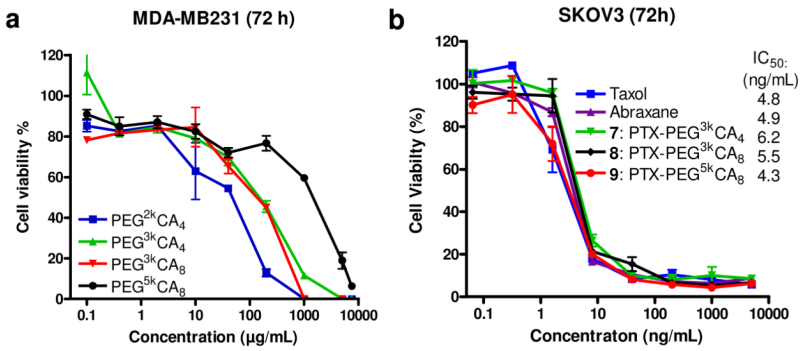

Figure 7.

(a) The cytotoxicity of empty telodendrimer micelles against the MDA-MB-231 breast cancer cells; no significant toxicity for PEG^{5k}-CA_8 was observed at 1 mg/mL concentration, telodendrimers with short PEG chains show moderate toxicity at high concentrations (50–150 μg/mL). (b) the tumor cell killing of the PTX loaded micelles in the SKOV-3 ovarian cancer cells, the very similar IC50 were observed for all the formulations in *in vitro* tumor cell killing.

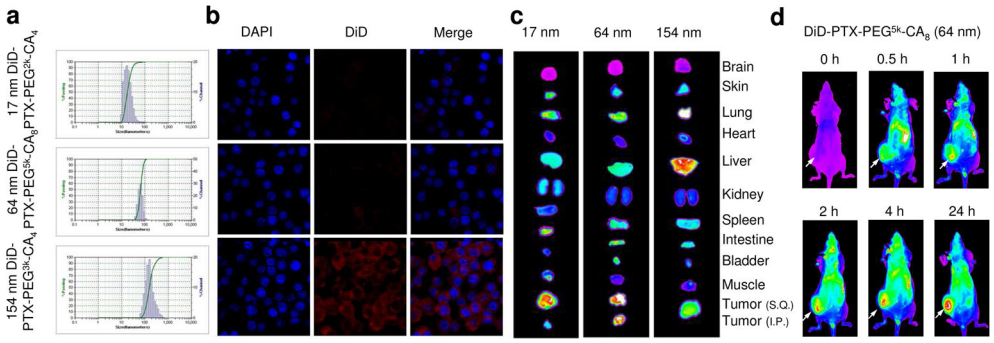

Figure 8.

(a) Three micelles, each with a different size after co-loaded with PTX and DiD, were measured with DLS particle sizer; (b) Raw 264.7 macrophage cells were incubated with each of the three micelle preparations, and then imaged under a confocal fluorescence microscope. The nuclei of the cells were stained with DAPI, the red DiD signals indicated that the 154 nm micelles, compared to the smaller micelles (17 nm and 64 nm) were preferentially taken up by the macrophages. (c) *ex vivo* biodistribution of the micelles (three different sizes) in the SKOV-3 ovarian cancer xenograft bearing mice at 24 h after tail vein injection; (d) *in vivo* NIR fluorescence imaging of the tumor bearing mice after i.v. injection with the DiD-PTX-PEG^{5k}CA$_8$ over time; passive accumulation of the micelles in the S.Q. implanted xenograft (arrow) was observed from 2 h to 24 h after injection.

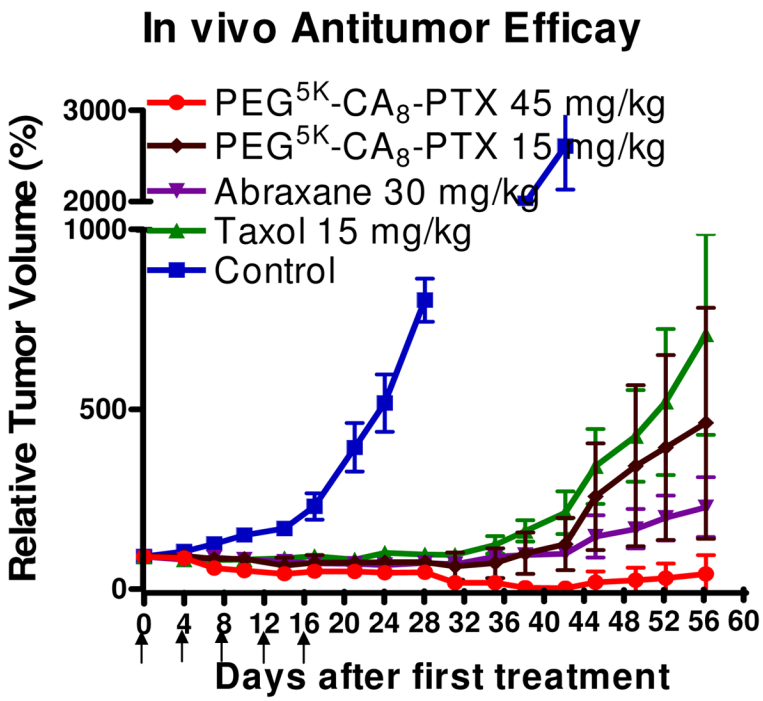

Figure 9.

Anti-tumor efficacy of different PTX formulations in nude mice bearing human SKOV3-luc ovarian cancer xenograft. PBS (control), Taxol, Abraxane and the PTX-PEG^{5k}-CA$_8$ preparations were administered i.v. on days 0, 4, 8, 12, and 16 (marked with arrows) when tumor volume reached about 50 mm^3.

Table 1

The physical properties of telodendrimers with different PEG chain length and the number of cholic acids and lipophilic molecules.

Telodendrimers	Mw (theo.)	Mw[a] (MS)	Mw[b] (NMR)	CMC (μM)[c]	Size (nm)[d]	Size with PTX (nm)[d]	PTX[e] (mg/mL)
PEG^{2k}-CA_4	3914	4105	4511	7.9	11.5	15	5.2
PEG^{3k}-CA_4	5250	5606	5251	12.5	15	141	5.6
PEG^{5k}-CA_4	6644	6313	6082	67	10	131	2.3
PEG^{2k}-CA_8	5986	5985	6127	1.3	302/6000	96/348/1863	N/D
PEG^{3k}-CA_8	7322	7624	8025	5.9	20	58	4.7
PEG^{5k}-CA_8	8716	8814	8805	5.3	21	61	7.3
PEG^{10k}-CA_{16}	8172	N/D	N/D	0.97	42.7/2163	102/602/2435	0.6
PEG^{5k}-CF_8[f]	8909	N/D	N/D	0.4	122/280/827	134/388/905	N/D
PEG^{5k}-LA_8[g]	8460	N/D	N/D	1.8	73/6000	67/450/872	0.8
PEG^{5k}-HA_8[h]	7620	N/D	N/D	1.5	55/322	97/5990	N/D

[a] Obtained via MALDI-TOF MS analysis, a-cyano-hydroxyl-cinnamic acid as a matrix compound.

[b] Obtained via ^{1}H NMR method. Given the molecular weights of the starting PEGs by MALDI-TOF MS (Figure S-1 in supporting information), the molecular weight was calculated based on the ratio of proton signals of the methyl groups on cholic acid to the proton signals of the PEG in the ^{1}H NMR spectra.

[c] CMC was measured by fluorescence spectrometry using pyrene (2×10^{-6} M) as a probe;

[d] Measured by dynamic light scattering particle sizer (Nanotrac®);

[e] PTX loading, in the presence of 20 mg/mL of telodendrimers, were measured by HPLC after passing through an 0.45 μm filter. N/D means not detectable;

[f] CF = cholesterol formate;

[g] LA = lithocholic acid;

[h] HA = heptadecanoic acid.